

Structure of polyethylene solid solutions: 2. Aspects of spectral deconvolution

D. J. Burchell and S. L. Hsu

Department of Polymer Science and Engineering, Material Research Laboratory, The University of Massachusetts, Amherst, Massachusetts 01003, USA

(Received 1 August 1980; revised 22 October 1980)

Several methods of factor analysis have been evaluated and applied to deconvolute the infra-red spectra obtained for solid solutions of binary mixtures of PE 2000 and PE 1000. In addition to the crystalline orthorhombic form, these spectroscopic techniques also reveal packing disorder in the form of a monoclinic phase. This packing disorder can be correlated with the amount of conformational disorder associated with these samples.

INTRODUCTION

Vibrational spectroscopic characterization of polymer conformation and molecular environment has mainly been based on normal coordinate and model compound analysis. However, when there is a mixture of conformations or a wide choice of environments, the structural information available in vibrational spectroscopy becomes much more difficult to assimilate. Thus, theoretical considerations are often further complicated by spectroscopic effects associated with inaccuracies in band position, halfwidth and intensity in conventional dispersive infra-red instruments. Therefore, polymer characterization is often an approximation particularly with regard to the determination of the number of contributing spectral components when several are present. Within the past few years Fourier transform infra-red spectroscopy, based on the use of Michelson interferometer and mini-computer, has made available accurate digitized spectroscopic information. The application of *FT* i.r. to the study of macromolecules has already led to significant findings with much promise for the future. In our laboratory we have been interested in the morphological characterization of melt crystallized polymer blends and stress deformation of semicrystalline polymers. The analysis of these spectral data often involves deconvolution of a given mixture spectrum into two or more independent contributing components that will regenerate the spectrum by linear combination. The analytical methods used in our laboratory include factor analysis¹⁻⁷ and the ratio method⁸.

This paper describes several general mathematical methods, incorporating estimates of measurement errors, to calculate and evaluate the number of species present in mixtures. Furthermore, we have applied these methods to analyse the structure of solid solutions of binary polyethylene mixtures, a model for extrudate¹. Our differential scanning calorimetry and low frequency Raman measurements have provided information regarding the distribution of extended chain length which arises from the large number of chain defects¹. For these samples we were also interested in examining another aspect of morphology, i.e. the possibility of packing defects. Factor analysis has proved to be quite valuable and the results are presented here.

EXPERIMENTAL

Polyethylene 1000 ($\bar{M}_n=980$, $\bar{M}_w/\bar{M}_n=1.1$) and polyethylene 2000 ($\bar{M}_n=1790$, $\bar{M}_w/\bar{M}_n=1.1$) were purchased from Polysciences Inc. All compounds were used without further purification.

Mixtures of PE 1000 and PE 2000 in various molar ratios were sealed in Pyrex tubes *in vacuo*. The sample tubes were heated to $\sim 15^\circ$ above the melting temperature of the higher melting component and were kept at this temperature with occasional shaking for approximately two h before quenching to liquid nitrogen temperature. All thermal and spectroscopic data were obtained immediately after quenching. The quenched mixtures have been shown to be solid solutions and their structures are reported elsewhere¹. These samples were kept at room temperature. A second analysis carried out one week later showed some structural changes.

Infra-red spectra ($4000\text{--}400\text{ cm}^{-1}$) were obtained on a Nicolet 7199 Fourier transform infra-red spectrometer. Two hundred scans at a resolution of 2 cm^{-1} were signal averaged and stored on a disc system. All the spectra stored are available for later analysis. Our spectral analysis computer programs are coded in Basic and can access the partial or entire spectrum of any particular data file on the magnetic disc system. In general, the infra-red spectra were obtained from KBr pellets containing 1.5% to 2.0% of quenched polyethylene mixtures. The criterion for the analysis is that Beer's law be obeyed, hence low absorptions are needed⁹⁻¹⁰.

Theory-factor analysis

As in the previous analyses²⁻⁷, a matrix A of $N_w \times N_s$ in dimension is formed from N_s , the number of mixture spectra, each containing N_w digitized absorption values, such that

$$A = N_w \begin{bmatrix} \text{spectrum 1} \\ \text{spectrum 2} \\ \vdots \\ \text{spectrum } N_s \end{bmatrix} \quad (1)$$

The spectral range to be considered, N_w , is flexible. Since the core storage in our computer is limited to 48K, depending on the number of mixtures to be considered, 2000–4000 data points is the usual computational limit. With our Nicolet 7199 FTIR, operating at 2 cm^{-1} resolution, zero filling once, corresponds to about 1 cm^{-1} per data point. So, for a 3000–1500 cm^{-1} region N_w is approximately 1500.

Several transformation methods of A and their effects have been summarized¹¹. In the present analysis, matrix A is baselined with a column matrix X , forming a new matrix Y , such that

$$Y = A - X \quad (2)$$

Each element of the i th column of X equals the absorbance minimum in the spectrum i over the frequency range represented by N_w . Then each spectrum can be viewed as being generated from the independent components of Beer's law

$$Y_{ij} = A_{ij} - X_j = \sum_{k=1}^{N_c} C_{kj} \epsilon_{ki} \quad (3)$$

where i corresponds to the wavelength, j to the mixture spectra, X_j is the minimum of spectrum j in the studied region C_{kj} is the concentration of species k in mixture j , ϵ_{ki} is the extinction coefficient of species k at wavelength i , N_c is the number of independent species.

The y matrix being the size $N_w \times N_s$ is too large to be conveniently analyzed. However, symmetric matrix B of size $N_s \times N_s$ can be defined by

$$B = Y^T Y \quad (4)$$

where Y^T is the transpose of Y . From matrix theory it can be shown that B is of the same rank as A or Y . The rank of this B matrix is important because it corresponds to the number of independent spectra needed to reconstruct the absorbance spectra. It should also be mentioned that the transformation of A to Y is a specific one of the more general form

$$Y = TA + Z \quad (5)$$

where T is a weighting matrix and Z is the adjustment matrix. In forming B , when each column is multiplied by a constant, there will be a change in the value of the eigenvalue but the number of non-zero eigenvalues or the number of contributing components, will remain unchanged. Therefore, an identity matrix can be used for T . Secondly, the adjustment of matrix Z can be formed from the average absorbance of the region³, or in this case the minimum absorbance of the region of interest. This second method is closest to the method usually used with Beer's law. In this formulation, there is only one zero absorbance at $(A_{ij})_{\min}$ and no negative values [note that this method is the same as the covariance about the origin method with the origin defined now as $(A_{ij})_{\min}$]. In contrast, the first method has a data set, $A_{ij} = A_{ij} - (A_{ij})_{\text{av}}$, therefore containing both positive and negative absorbance values, which is inconsistent with Beer's law. Secondly, the negative values are given undeserved weight when the Y matrix is premultiplied by its transpose in forming B .

A convenient method to determine the rank of B is to search the number of 'non-zero' eigenvalues²⁻⁷. However, in each of these searches, there are computational inaccuracies and more importantly measurement inaccuracies, resulting in none of the eigenvalues being identically zero. What is necessary, therefore, is a statistical criterion for the 'vanishing' of an eigenvalue. In most cases the real eigenvalues are usually significantly larger than the error eigenvalues (which are usually the same order of magnitude), so a qualitative comparison will reveal the actual number of non-zero eigenvalues or the rank of the matrix B^2 . In cases where this criterion fails to distinguish clearly the actual eigenvalues from the error eigenvalues, we have incorporated three additional criteria in our analysis to determine which eigenvalues are in fact non-zero.

Since B matrix is real and symmetric, it can be expressed as follows:

$$B = \lambda_1 v_1 v_1^T + \lambda_2 v_2 v_2^T + \dots + \lambda_n v_n v_n^T \quad (6)$$

where λ_i and v_i are the i^{th} eigenvalue and normalized eigenvector, respectively and n is the number of non-zero eigenvalues. Then in the actual analysis, another B matrix $B1$, can be constructed from the computed eigenvalues and eigenvectors as follows:

$$B1 = \sum_{i=1}^k \lambda_i v_i v_i^T \quad (7)$$

As an alternative criterion, the minimum k that satisfies the following

$$B - B1 \leq 0.001 * B \quad (8)$$

or

$$B_{ij} - B1_{ij} \leq 0.001 B_{ij} \quad (9)$$

for each element of the two matrices will be considered as the rank of the B matrix.

The standard deviation of the absorbance for k components, S_k , is defined by⁵:

$$S_k = \frac{1}{N_s} \left(\frac{\text{Tr}(B) - \sum_{i=1}^k \lambda_i}{N_w - k} \right)^{1/2} \quad (10)$$

where $\text{Tr}(B)$ is the trace of B . Let the estimated error of the absorbance measurements be S_a .

This third criterion in determining the rank of B is to search for the minimum k such that $S_k \geq S_a \geq S_{k+1}$. The measurement error depends on a number of experimental parameters and the energy available at the detector as a function of frequency. This can be seen from the 100% line shown in Figure 1. For our analysis, the estimated error of the absorbance measurement is taken to be the maximum absorbance deviation from 0.0 for the frequency region of interest.

The fourth criterion to determine the non-zero eigenvalues can be arrived at via an estimation of the square root of the variance, σ_i , of each eigenvalue, incorporating possible measurement error³. If the computed eigenvalues are arranged in order of decreasing value, then only the eigenvalues larger than their standard errors will be considered as significant. For the eigenvalues smaller than their standard errors, they should therefore be

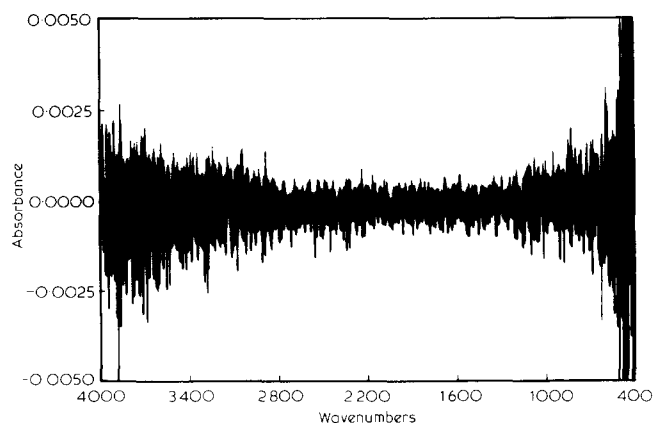


Figure 1 100% line through KBr pellets; 100 scans at 2.0 cm⁻¹ resolution

Table 1 Results of factor analysis on xylene mixtures (1700–1300 cm⁻¹). Max. of 100% ABS. spectrum from 1700–1300 cm⁻¹ = 3.66E-3

Number	RSD *	Eigenvalue	σ^\dagger
1	0.06512	27.7463	2.98478E-2
2	3.79918E-2	1.16185	2.24579E-2
3	6.65759E-3	0.57902	2.46007E-2
4	2.54667E-3	1.56274E-2	2.73238E-2
5	7.24201E-4	2.45552E-3	2.33666E-2
6	4.26543E-4	1.40928E-4	3.30068E-2
7	1.98402E-4	5.84988E-5	2.34154E-2

* RSD – Residual standard deviation

† σ – Square root of the variance of each eigenvalue

regarded as being statistically equivalent to zero. In an analysis, the order is taken as k when:

$$\begin{aligned}\lambda_k &> \sigma_k \\ \lambda_{k+1} &< \sigma_{k+1}\end{aligned}\quad (11)$$

Again, in this method the estimated error associated with each frequency is taken from the 100% line.

DISCUSSION

As an example of applying these statistical methods to analyse mixture spectra, *ortho*-, *para*- and *meta*-xylene solutions in various compositions were prepared to be used as a model system. The 1300–1700 cm⁻¹ region was selected for analysis. In this region the maximum absorbance deviation from 0.0 for the 100% line is approximately 3.66×10^{-3} . The computed residual standard deviation, eigenvalues and the square root of variance are shown on Table 1. For this model system it is clear that all four methods yield the result that the seven mixtures arise from three independent spectra¹². One should notice the relative magnitudes of the third and fourth eigenvalues. In addition, the residual standard deviation associated with the third eigenvalue is clearly above the possible error. In contrast, the standard deviation of the fourth largest eigenvalue is smaller than the error. Similarly, the significance of the first three eigenvalues are easily seen when the square root of the variance is considered. Only these three eigenvalues are sufficiently large to be considered as real.

Raman spectroscopy and differential scanning calori-

metry have revealed interesting morphological features associated with polyethylene 1000 and 2000 binary mixtures; namely, the existence of considerable conformational disorder¹, the degree of which depends on composition. Ott and Slagle¹³ first raised the possibility that aliphatic chains in solid solutions of fatty acids may exist both fully extended and as non-extended chains. This model is consistent with that analysis. Furthermore, it was found that the composition containing 71 mol % of PE 2000 contains the greatest number of nonextended chain segments. The natural question is whether the statistical methods presented previously can be used to elucidate additional morphological features. Based on earlier theoretical normal coordinate analysis, the vibrational spectrum of polyethylene is understood in great detail^{14–15}. The bands listed in Table 2 are characteristic of particular chain conformation and packing^{14–19}. Indeed, the difference spectra obtained for samples freshly prepared and one week later revealed substantial differences in the 1400 and 700 cm⁻¹ regions. This is shown in Figures 2 and 3. Specific changes are seen in the 1475 cm⁻¹ and 717 cm⁻¹ bands which are assigned to the CH₂ bending and CH₂ rocking of polyethylene. It is known these bands are particularly sensitive to chain conformation and packing changes^{14–16}.

The results of the factor analysis carried out for the 680–800 cm⁻¹ region of the samples of varying composition are shown in Table 3. Unlike the xylene case, the number of independent components contributing to the spectra cannot be easily obtained. For the quenched material, the comparison of eigenvalues and the evaluation of the residual standard deviation does not show clearly two or three independent components. The residual standard deviation of the third eigenvalue is comparable to the error estimate. However, the reconstruction of the *B* matrix and the evaluation of the square root of variance (our most favoured method) have shown that there are only two linearly independent components to the spectra obtained. For the spectra containing two linearly independent components, the 'ratio method' can be used to deconvolute the two spectral contributions⁸. In the CH₂ rocking region, one of the components is determined to be

Table 2 Band frequency assignment for particular chain conformation and packing

Frequency (cm ⁻¹)	Assignment	Reference
717	CH ₂ rock in a monoclinic crystal phase	16
720	In-phase CH ₂ rock crystal and amorphous phases	17
730	Out-of-phase CH ₂ rock crystal phase	17
1078	Skeletal C–C stretch amorphous phase	18
1308 and 1368	CH ₂ wag in <i>GTG</i> or <i>GTG'</i> amorphous phase	14
1352	CH ₂ wag in <i>GG</i> amorphous phase	14
1475	CH ₂ bending of the monoclinic phase	16
1894	Combination of Raman active 1168 and 720–730 i.r. bands crystal phase	19
2016	Combination of Raman active 1295 and 720–730 i.r. bands crystal and amorphous phases	19

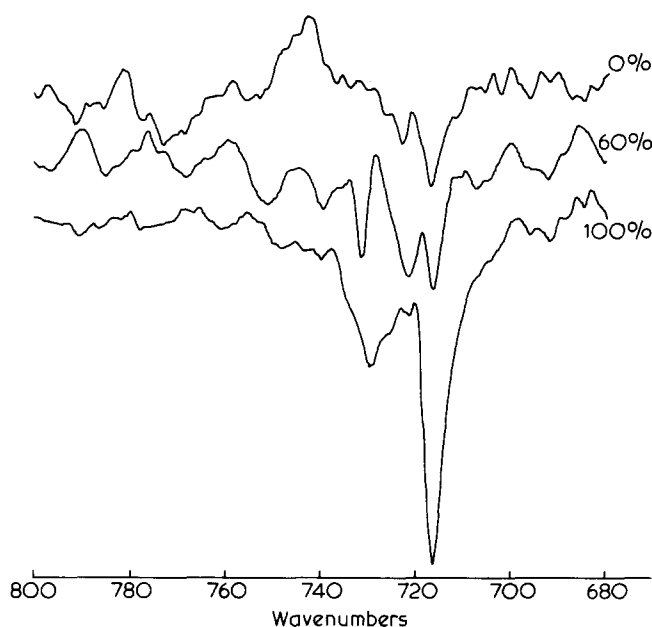


Figure 2 Difference spectra of the annealed — as quenched polyethylene solid solutions in the CH_2 rocking region. Numbers refer to the molar concentration of PE2000. Percentages listed are mol% 2000 in binary mixtures of polyethylene 1000 and 2000. Y axis scaled at 0.007 ABS

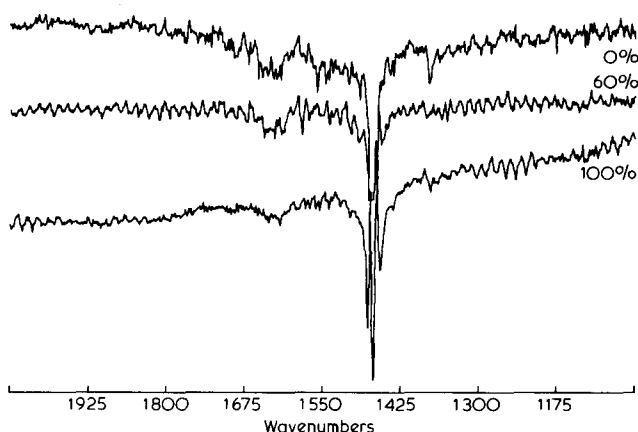


Figure 3 Difference spectra of the annealed — as quenched polyethylene solid solutions in the CH_2 bending region. Numbers refer to the molar concentration of PE2000. Percentages listed as in Figure 2 and Y axis scaled as Figure 2

the characteristic $720\text{--}730\text{ cm}^{-1}$ doublet of the CH_2 rocking vibration arising from the crystal-field splitting for chains packed in an orthorhombic unit cell¹⁵. The other components consist of a band at 717 cm^{-1} with a broad band between 720 and 730 cm^{-1} . The integrated intensity for this second component is sensitive to the composition of the binary mixture. The broad band is assignable to the polyethylene in the amorphous phase. The 717 cm^{-1} band must arise from CH_2 rocking vibration since no other fundamental mode is known to be in this region¹⁴. Paraffin or polyethylene samples subjected to various thermal, chemical or mechanical treatments have often shown a band from $715\text{--}717\text{ cm}^{-1}$. The most reasonable assignment is the CH_2 rocking vibration which arises from polyethylene chains packed in the monoclinic unit cell¹⁶. However, this kind of defect does not imply long lateral order necessary to be seen by X-ray diffraction¹⁶. In this structure, the interchain non-

bonded interactions are significantly weaker than in the orthorhombic unit cell, therefore only one component of the CH_2 rocking doublet can clearly be observed. In addition to the conformational defects measured by Raman and differential scanning calorimetry on solid solutions of binary mixtures, a new aspect of their morphology, i.e. a considerable but varying amount of packing defects has been observed.

The amount of the monoclinic phase varies with composition similar to the conformational disorder and their exact relationship is of interest. The crystallinity of the mixtures is estimated by measuring the peak area for the heat of fusion ($\Delta H_f = 3.37\text{ kJ mol}^{-1}$ for PE 1000 and 3.60 kJ mol^{-1} for PE 2000)¹¹. The degree of crystallinity measured is between 65–80%. Since the $720\text{--}730\text{ cm}^{-1}$ doublet arises from interchain interaction in the crystalline regions, a relationship between the integrated intensity of these two bands and the degree of crystallinity is expected. This is shown to be true for the composition measured in Figure 4. In addition, the amount of conformational disorder has been estimated by the normalized integrated intensity of the longitudinal acoustic mode for these samples¹. These values show a similar composition dependence over the range measured as the integrated intensity of the 717 cm^{-1} band. This is shown in Figure 5. It should be emphasized that the above similarities are indicative of trends, the exact relationship has not been developed. This important aspect is the subject of current study.

CONCLUSION

Four methods of factor analysis have been evaluated. Although each is satisfactory for model systems, in some cases, the results derived from one or more methods may not be conclusive in assigning the number of components in polymer spectroscopy. However, as a whole, the number of linearly independent components in a set of mixture spectra can usually be assigned. This analytical method applied to several solid solutions of polyethylene binary mixtures of varying composition revealed two independent components. In the CH_2 rocking region, one component is the $720\text{--}730\text{ cm}^{-1}$ band associated with the polyethylene chains packed in an orthorhombic unit cell. The second component consists of a 717 cm^{-1} band and a

Table 3 Results of factor analysis on polyethylene mixtures ($800\text{--}680\text{ cm}^{-1}$). Max. of 100% ABS. spectrum from $800\text{--}680\text{ cm}^{-1} = 1.32\text{E-}3$

Number	RSD	Eigenvalue	σ
1	5.33847E-3	1.54496	2.96482E-3
2	3.12712E-3	8.34519E-3	3.58837E-3
3	1.45463E-4	9.48117E-4	3.59177E-3
4	7.55064E-4	1.89860E-4	2.93054E-3
5	5.57710E-4	3.17762E-5	2.61072E-3
6	3.32547E-4	2.42556E-5	3.06154E-3
7	2.06737E-4	8.14703E-6	2.59610E-3
8	6.33299E-8	4.99877E-6	2.48753E-3
1	4.41508E-3	1.41556	2.67400E-3
2	2.18890E-3	6.54341E-3	2.99964E-3
3	1.11117E-3	4.40300E-4	2.45549E-3
4	8.34397E-4	6.66353E-5	3.13053E-3
5	5.94120E-4	4.20417E-5	2.88239E-3
6	3.80771E-4	2.51964E-5	2.88282E-3
7	2.53480E-4	9.70637E-6	2.53945E-3
8	4.84287E-8	7.56076E-6	2.88192E-3

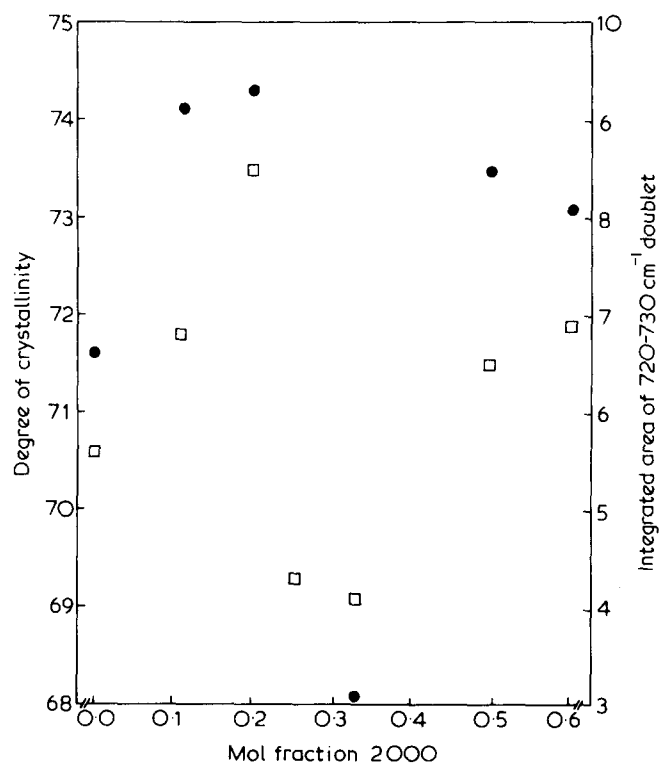


Figure 4 Comparison of crystallinity with the integrated area of the deconvoluted 720–730 cm^{-1} doublet as a function of composition, where ● corresponds to d.s.c. crystallinity measurements and to the integrated area of the 720–730 cm^{-1} doublet

broad band between 720 and 730 cm^{-1} . These two bands can be assigned to the chains in monoclinic phase and the amorphous phase respectively. The integrated intensities of the bands correlate well to the degree of crystallinity and conformational disorder measured by thermal analysis and Raman spectroscopy.

ACKNOWLEDGEMENT

This research was supported by National Science Foundation Grant No. 79-02883 and the Materials Research Laboratory of the University of Massachusetts.

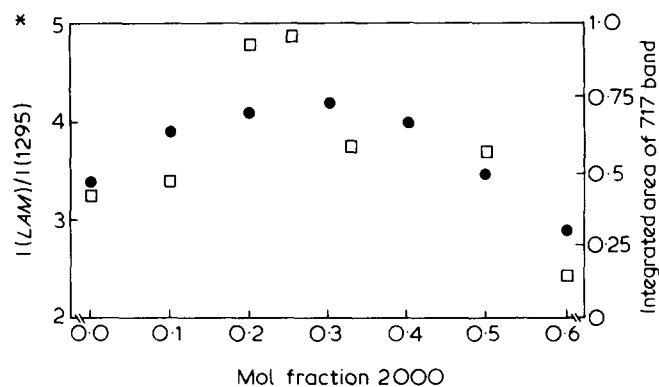


Figure 5 Comparison of the integrated area of the 717 cm^{-1} component with the integrated intensity of the longitudinal acoustic mode observed for the polyethylene solid solutions where ● corresponds to the $I(\text{LAM})/I(1295)$ values from reference 1* and □ to the integrated area of the 717 cm^{-1} band

REFERENCES

- Shu, P. H. C., Burchell, D. J. and Hsu, S. L. *J. Polym. Sci. Polym. Phys. Edn.* 1980, **18**, 1421
- Antoon, M. K., D'Esposito, L. and Koenig, J. L. *Appl. Spectrosc.* 1979, **33**, 351
- Hugus, Z. Z. Jr. and El-Awady, A. A. *J. Phys. Chem.* 1971, **75**, 2954
- Blackburn, J. A. *Anal. Chem.* 1965, **37**, 1000
- Kankare, J. J. *Anal. Chem.* 1970, **42**, 1322
- Ritter, G. L., Lowry, S. R., Isenhour, T. L. and Wilkins, C. L. *Anal. Chem.* 1976, **48**, 591
- Bulmer, J. T. and Shurvell, H. F. *J. Phys. Chem.* 1973, **77**, 256
- Koenig, J. L., D'Esposito, L. and Antoon, M. K. *Appl. Spectrosc.* 1979, **31**, 292
- Antoon, M. K., D'Esposito, L. and Koenig, J. L. *Appl. Spectrosc.* 1979, **33**, 349
- Strassburger, J. and Smith, I. T. *Appl. Spectrosc.* 1979, **33**, 283
- Rozett, R. W. and Peterson, E. M. *Anal. Chem.* 1975, **47**, 1301
- Antoon, M. K., Koenig, J. H. and Koenig, J. L. *Appl. Spectrosc.* 1977, **31**, 518
- Ott, E. and Slagle, F. B. *J. Am. Chem. Soc.* 1933, **55**, 4404; *J. Phys. Chem.* 1933, **37**, 257
- Snyder, R. G. *J. Chem. Phys.* 1967, **47**, 1316
- Tasumi, M. and Krimm, S. *J. Chem. Phys.* 1967, **46**, 755
- Painter, P. C., Havens, J., Hart, W. W. and Koenig, J. L. *J. Polym. Sci. Polym. Phys. Edn.* 1977, **15**, 1237
- Stein, R. S. *J. Chem. Phys.* 1955, **23**, 734
- Krimm, S. *Fortschr. Hochpolym.* 1967, **47**, 1316
- Nielson, J. R. and Woollett, A. H. *J. Chem. Phys.* 1957, **26**, 1391